Preparation and characterization of halide materials for scintillators and lasers

R. Král[1], J. Pejchal[1], P. Zemenová[1,2], A. Bystřický[1], V. Jarý[1], M. Buryi[1], M. Salomoni[3], E. Auffray[3], M. Nikl[1]

[1] Institute of Physics CAS, Prague, Czech Republic

[2] UCT Prague, Prague, Czech Republic

[3] CERN, Geneva, Switzerland

Hygroscopicity halides

= "absorbing or attracting moisture from the air"

physical adsorption

- Van der Waals forces
- fast (seconds)

chemisorption

- reaction
- formation of new compounds
- thermodynamics and kinetics

Formation of compounds

- hydrates — $MX.xH_2O$
- hydroxy-halides — $MOH.MX$
- oxy-halides — $MO.MX$

Kinetics defines ⬇ hygroscopicity

low X **high**

$$PbCl_2 + H_2O \rightarrow Pb(OH)Cl + HCl$$

$$2Pb(OH)Cl \xrightarrow{170°C} PbCl_2 \cdot PbO + H_2O$$

H. Podsiadlo, J. Therm. Anal. 37 (1991) 613–626.

Influence on wettability of melt

Impurities

- presence of O^{2-}, OH^{-}, CO_3^{2-}, etc.
- melt WETS ampoule surface
- may lead to ampoule and crystal cracking

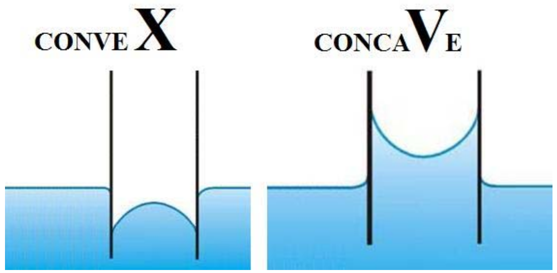

Shape of meniscus

impurities

NO impurities

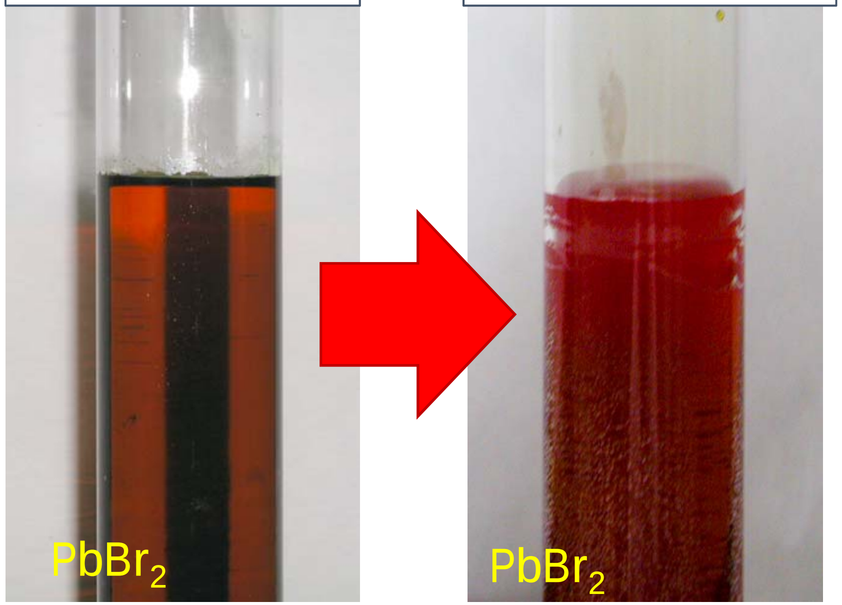

concave meniscus

convex meniscus

Principle of scintillators

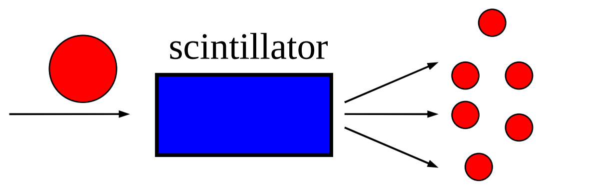

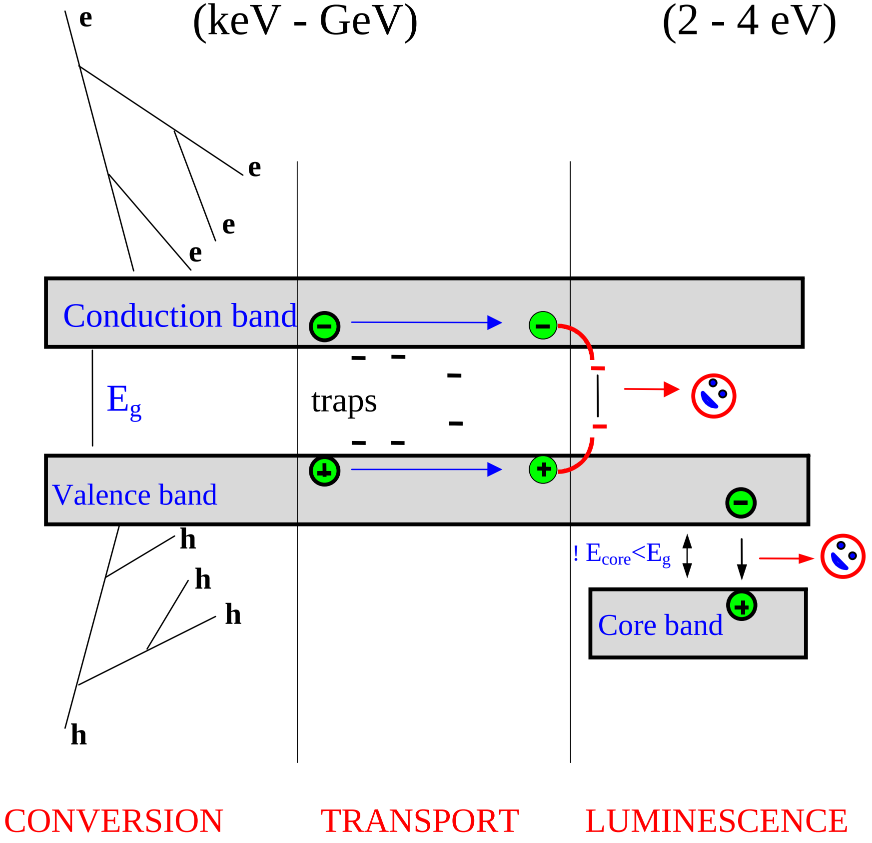

Scintillators

– detectors of radiation

– convertors the energy of ionizing radiation into VUV/UV/visible light

Application

- medical imaging, homeland security, high energy physics, etc.

Transport

– shallow traps/defects influence transport of charge carriers to luminescence centers

– slow components in the scintillation decay

Removal of oxidic impurities in halides

various methods: extraction, melt filtration, etc.

Chemical pur.

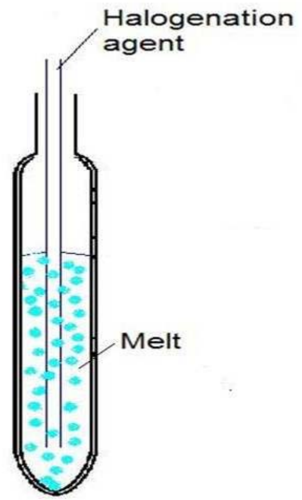

- reactive agents into melt of halides
- based on: HX, X_2, CX_4, SiX_4
- anionic purification

Physical pur.

= zone refining

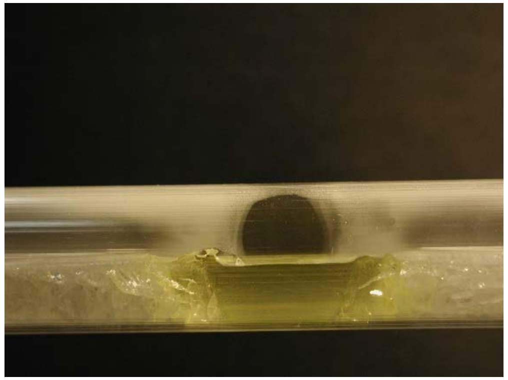

- 20 to 40 passes
- zone travel rate 25 mm/h
- $k_0 < 1$, $k_0 > 1$, $k_0 = 1$
- cationic purification

Ternary alkali metal halides

general formula

$$A_2MX_6 = 2\,AX + MX_4$$

A = Li, Na, K, Rb, Cs

M^{4+} = Ti, **Zr**, **Hf**, Pt, Sn, Se, Te

X = F, Cl, Br, I

	Cs_2HfCl_6
m.p. [°C]	826
Melting	congruent
Phase transition [°C]	no
Density [g/cm^3]	3.8
Crystal. structure	cubic
Space group	Fm-3m

doping

$(UO_2)^{2+}$, Te^{4+}, Sn^{4+}, Re^{4+} Os^{4+}, Mo^{3+}, Ir^{4+}, Na^{+}, Ce^{3+}, Eu^{2+}

Application of Cs_2HfCl_6

- ✓ as cost-effective radiation detector (scintillators)
- ✓ highly proportional light yield
- ✓ even without doping with any intentional activator

Properties

	Cs_2HfCl_6	Tl:NaI	Tl:CsI	$Eu:SrI_2$	$Ce:LaBr_3$
Density [g/cm^3]	3.8	3.4	4.5	4.6	5.3
m.p. [°C]	826	661	621	538	783
Cryst. structure	Cubic	Cubic	Cubic	Orthorhom.	Hex.
Eg [eV]	6.3	5.8	6.1	5.5	5.9
Zeff	58	50	51	49	47
Emission max. [nm]	380	410	540	430	360
Decay time [ns]	300 (5%); 4,4 (95%)	230	1100	600-2400	35
Light yield [ph/MeV]	54,000	38,000	66,000	80,000-120,000	61,000
Resolution [%] @662 eV	3-4	7	6	3-4	3
Hygroscopicity	no	yes	yes	yes	yes

synthesis

Starting materials

- CsCl, pre-purified
- $HfCl_4$, 3N, Zr < 0.5 %

Glovebox (Ar, H_2O, O_2 < 0.5 ppm)

- handling, weighing – CsCl, $HfCl_4$
- $HfCl_4$ – hygroscopic

Direct reaction

$$CsCl\ (l) + HfCl_4\ (g) = Cs_2HfCl_6\ (s,l)$$

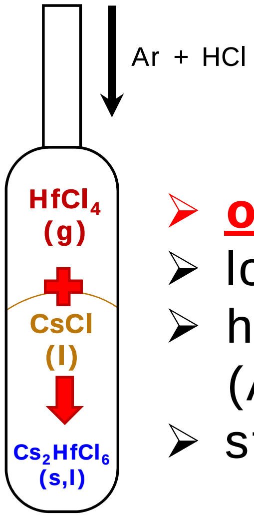

- **opened system**
- losses of $HfCl_4$ -> subl.
- hal. agents (Ar, HCl)
- start. charge 40g

- **closed system**
- $HfCl_4$ resubl.
- vacuum
- start. charge 100g

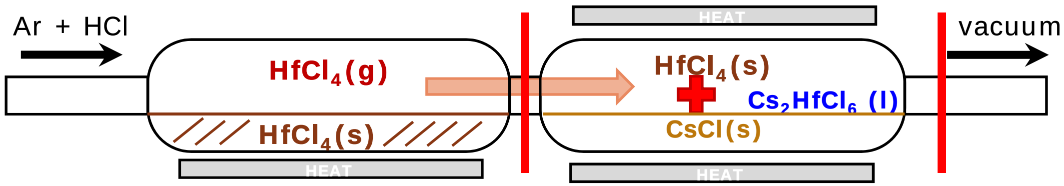

purification

Zone refining

- 20 to 40 passes
- zone travel rate up to 30 mm/h

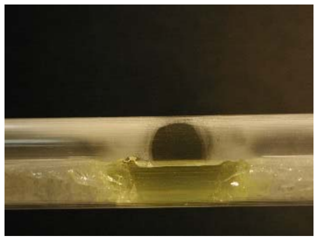

Asvestas et al. Can. J. Chem. 55 (1977) 1154.

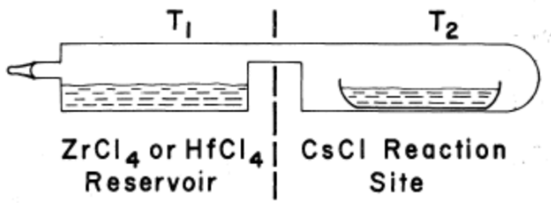

320 °C 475 °C

Crystal growth by **vertical Bridgman method**

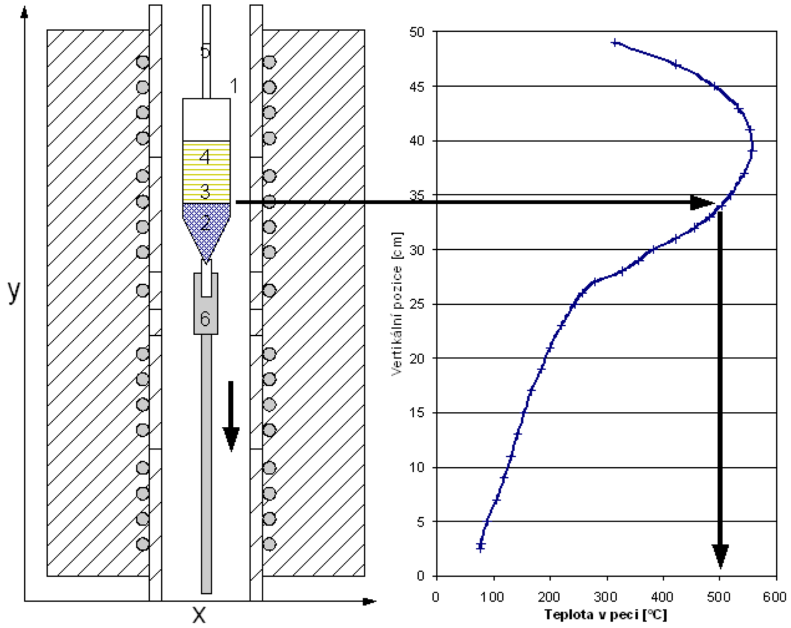

(a) (b)

- Resistive furnace (2 segments)
- Container = **quartz ampoule**
- No seed
- pulling rate **0,2 - 1,0 mm/h**
- Temperature gradient **30 - 40 K/cm**
- Cooling rate **12 K/h**
- **10 days (heating, growth, cooling)**

Characterization

Zone refining

- X-ray fluorescence analysis (XRF)
- X-ray diffraction analysis (XRD)

Crystal growth

- Thermogravimetry and differential scanning calorimetry (TG-DSC)
- Absorption (ABS)
- Radioluminescence (RL)
- Photoluminescence (PL, PLE), PL decay
- Light yield (LY)

Results - XRD

After zone refining

- opened x closed

used for CRYSTAL GROWTH

System	Phase	1	2	3	4	5
Opened	Cs_2HfCl_6	69.				
	CsCl	30.				
	-	-				
Closed	Cs_2HfCl_6	52.				
	CsCl	47.				
	$HfOCl_2.6H_2O$	-				

* in mol%

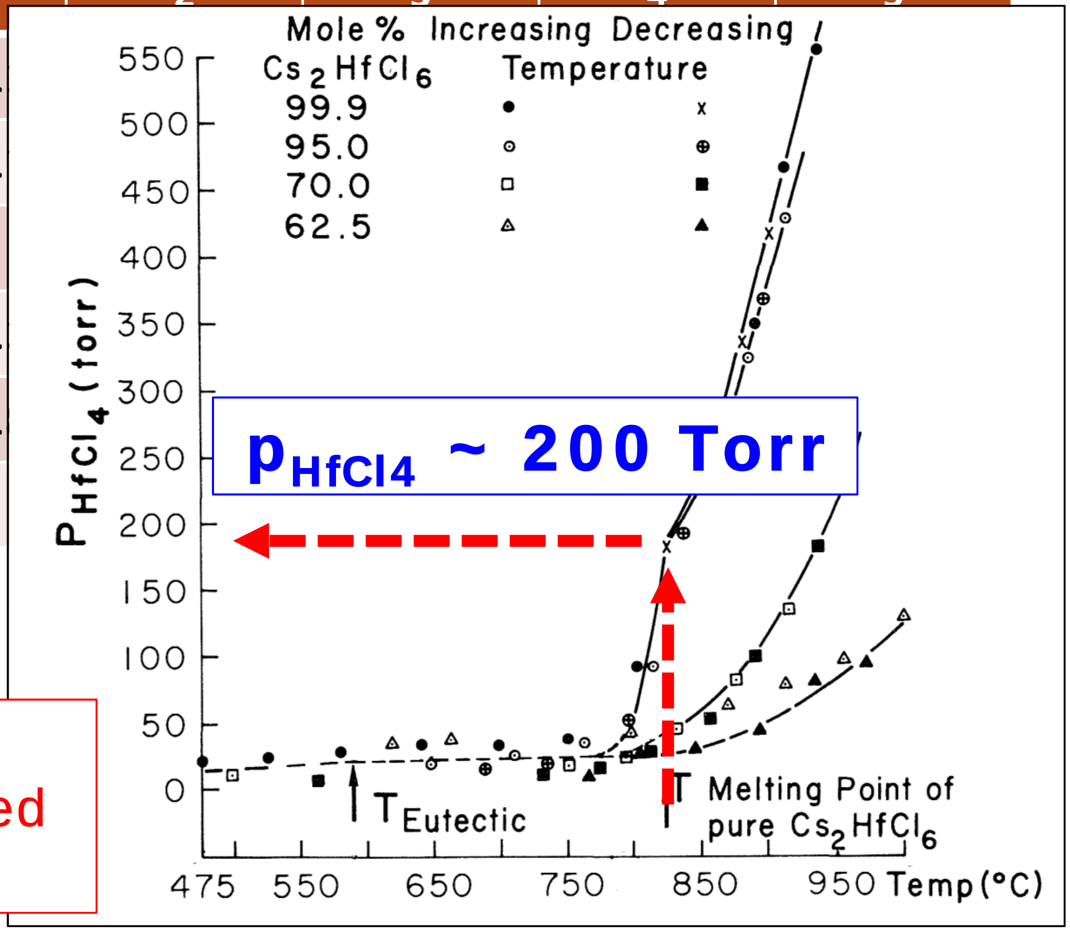

Cs_2HfCl_6
- unable to zone refined
- decomposed

Asvestas et al. Can. J. Chem. 55 (1977) 1154.

TG-DSC - Cs_2HfCl_6, single crystal, START

Theor. decomp. **-49 wt%**
$Cs_2HfCl_6 \rightarrow 2\ CsCl + HfCl_4$

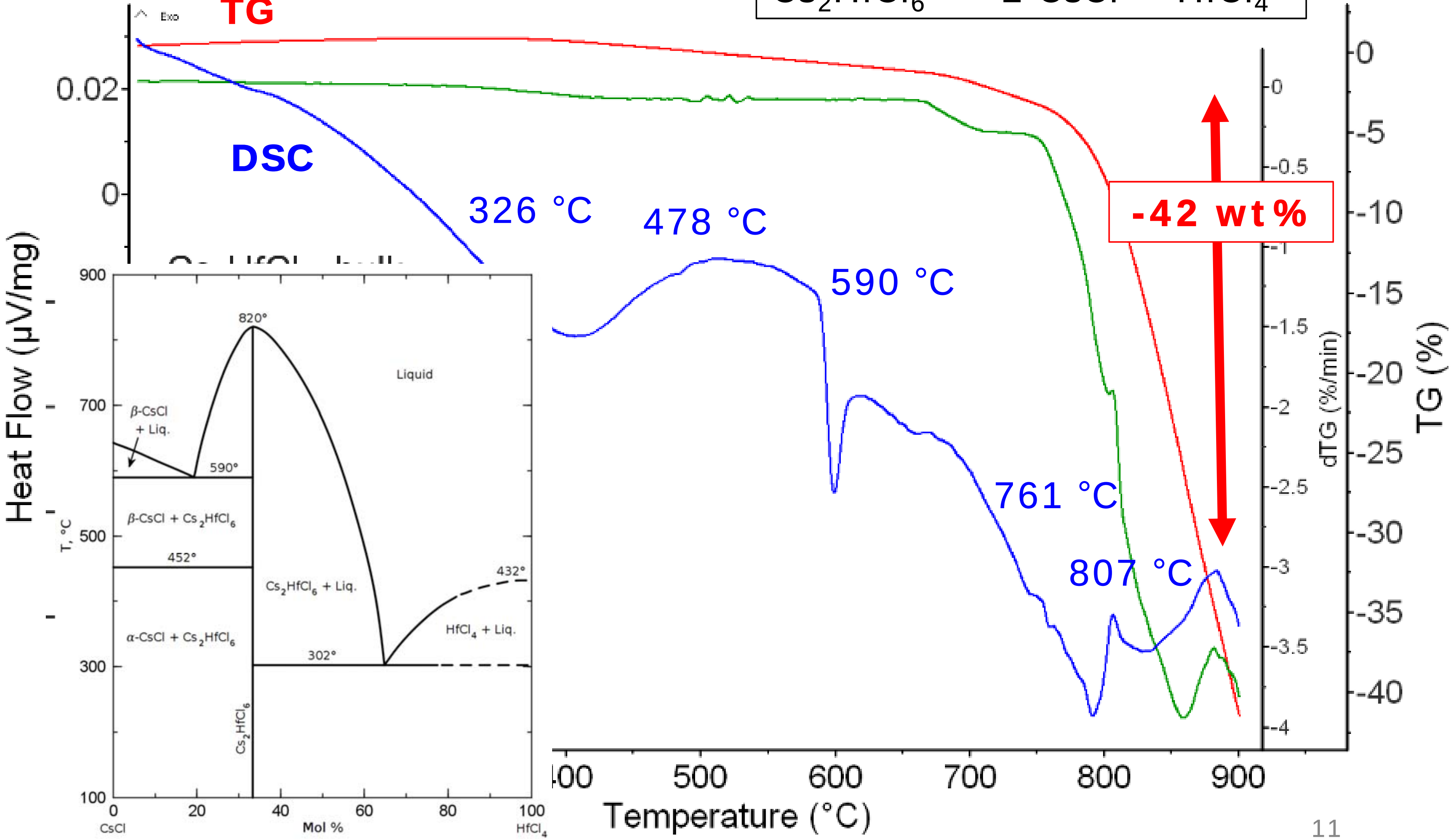

As-grown Cs_2HfCl_6 crystal

- vertical Bridgman growth
- charges of Cs_2HfCl_6 from opened system: 2, 3, and 4
- 12 x 40 mm (D x L), colorless
- polycrystalline, homogeneous grains
- tip and bulk – transparent
- tail – nontransparent

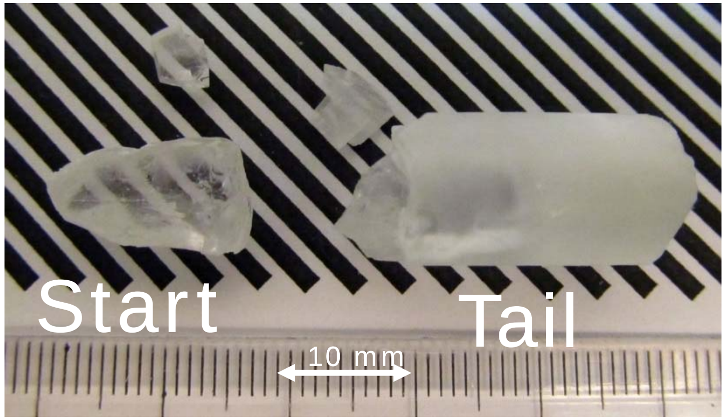

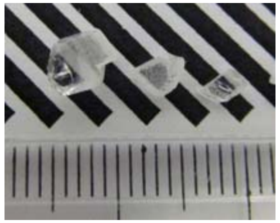

- ➢ Cleaved samples
- ➢ direction <111>

XRD

Comp.	Start [mol%]	Tail [mol%]
Cs_2HfCl_6	97	22
CsCl	3	78

Cs_2HfCl_6, single crystal, START

Radioluminescence, RT

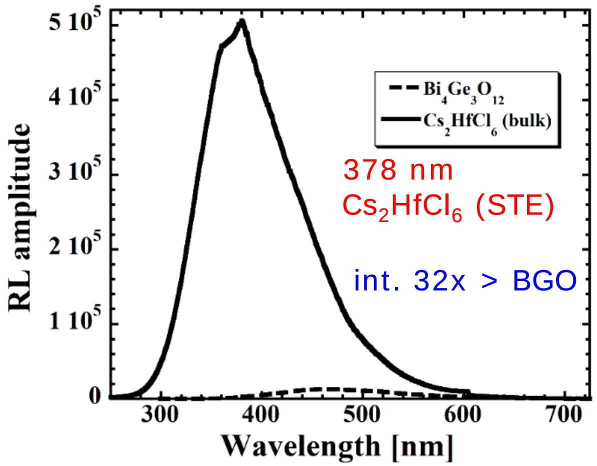

PL, PLE spectra, RT

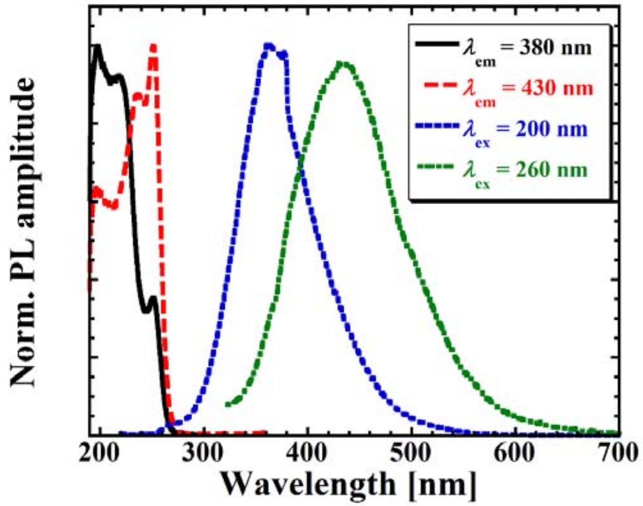

Absorption, RT

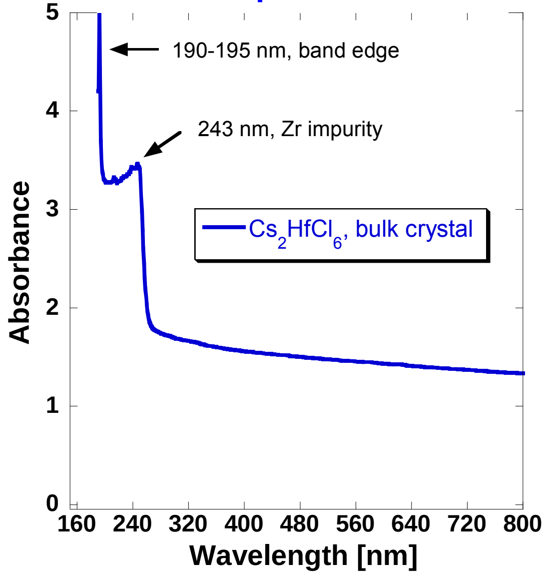

- ✓ band edge 195 nm -> band gap 6.3 eV
- ✓ Zr absorption 243 nm

- ✓ **360 nm** – em. of STE in Cs_2HfCl_6, PL decay **4.4** μs
- ✓ **440 nm** – em. of STE of Zr impurity, PL decay **12.0** μs

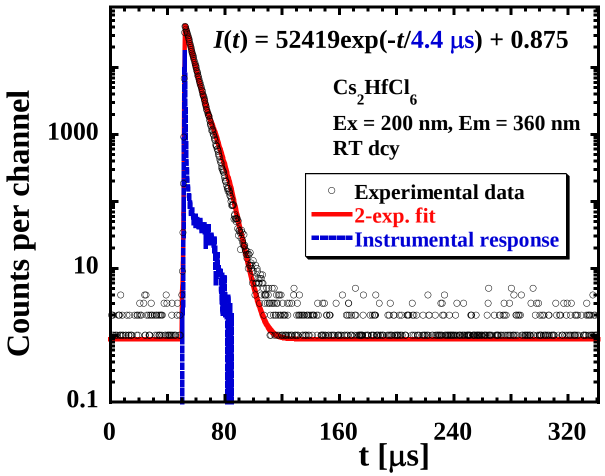

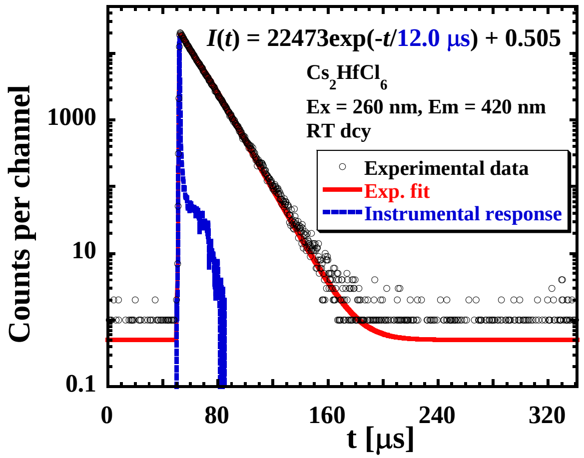

Electron paramagnetic resonance (EPR), Cs_2HfCl_6

R. Kral et al., J. Phys. Chem. C, 121 (2017) 12375−12382.

2x V_k centers identified:

- $V_k(a)$ = Cl_2^-, [110]
- $V_k(b)$ = interstitial Cl_2^-, [100]

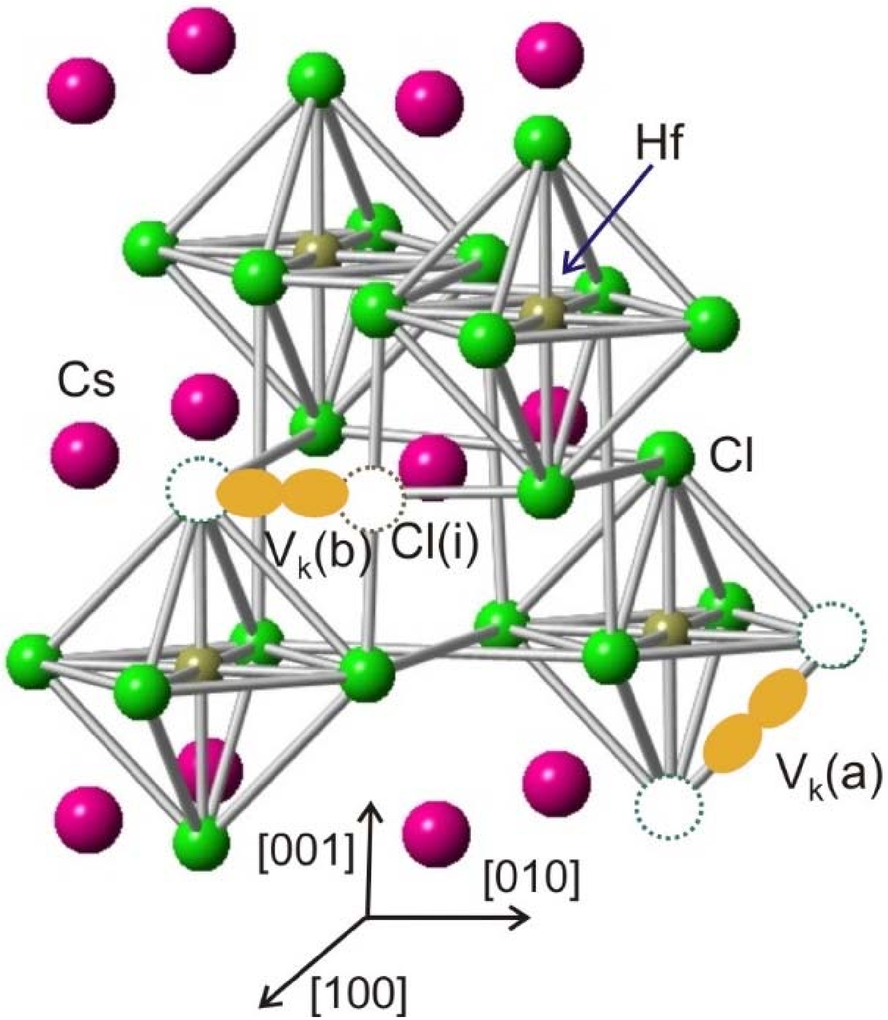

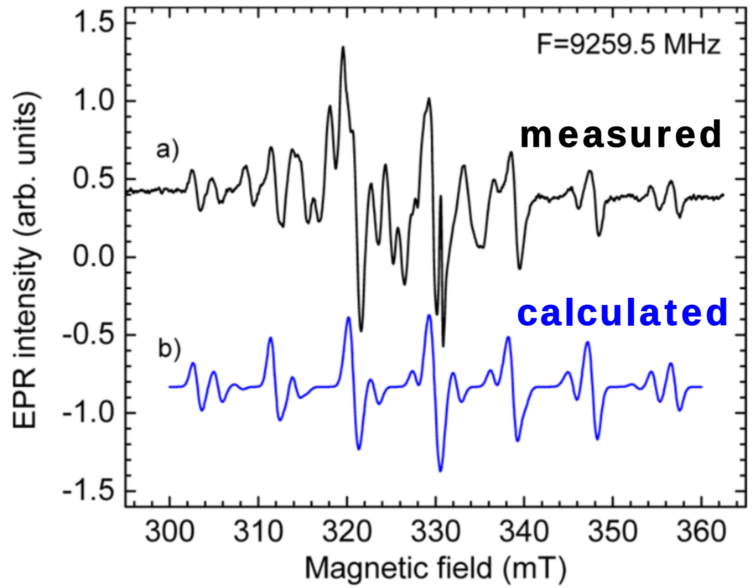

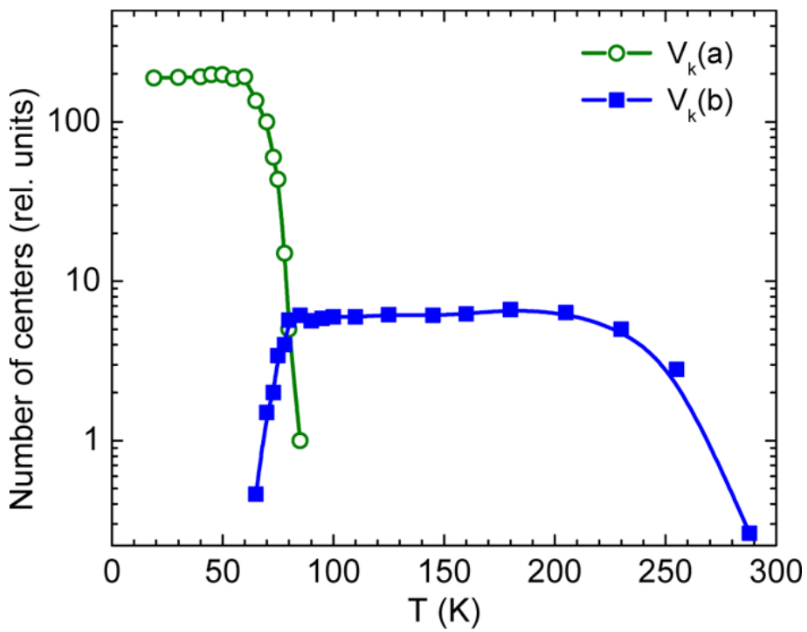

Light yield

- ^{137}Cs source, 20 us gate
- no optical coupling with grease
- teflon “blanket”
- $(Lu,Y)_2SiO_5:Ce$ (LYSO) crystal as standard

- **hygroscopic?** – reacted on atm.

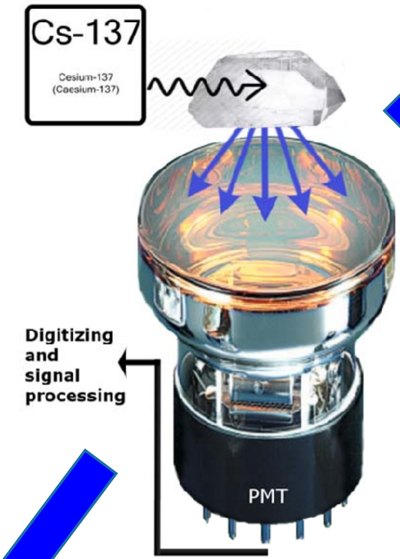

Cs_2HfCl_6, bulk crystal

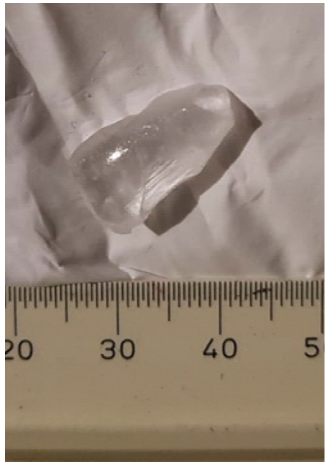

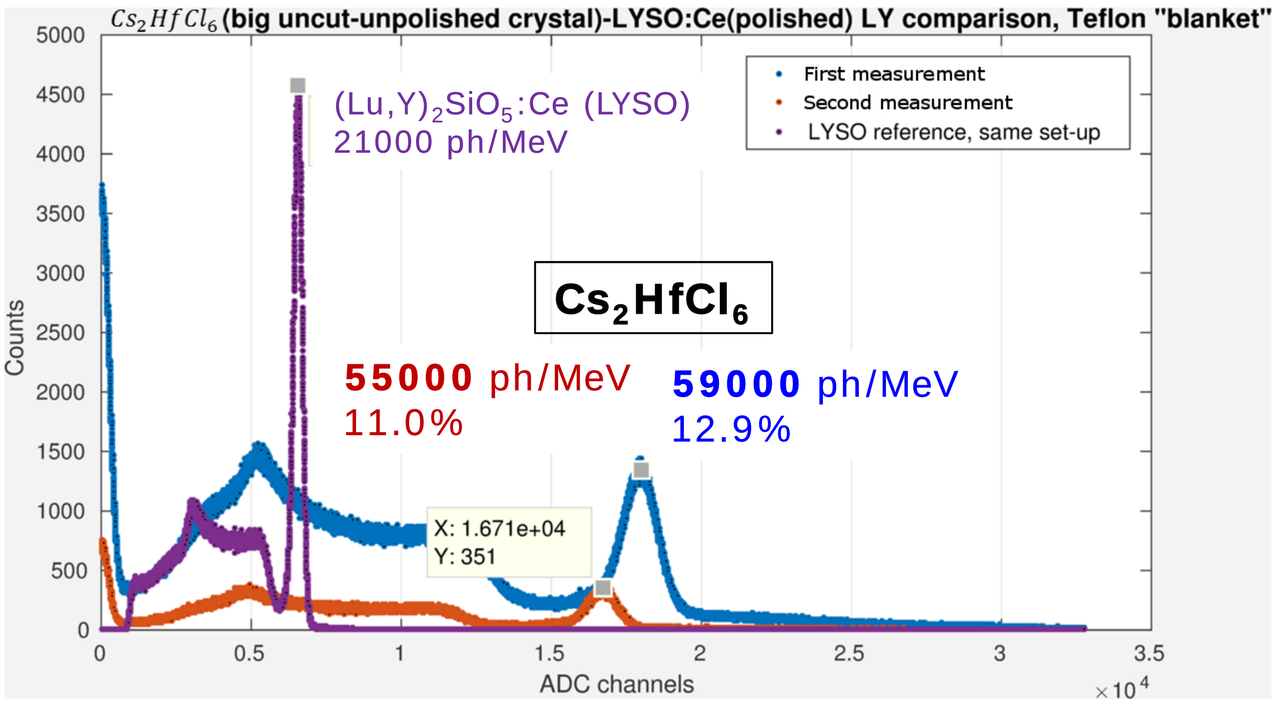

Excitation under UV:

- 365 nm (top)
- 254 nm (bottom)

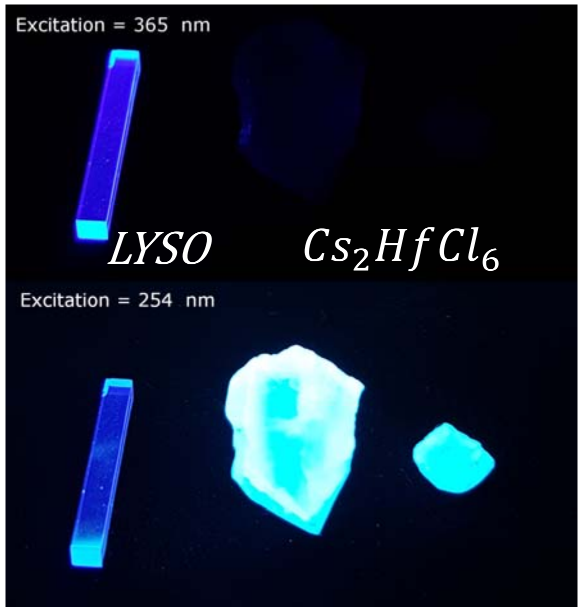

Halide mPD method

Prep and purif. of **starting material** + dop. el. (RE)

↓

Setting hot zone + material in glovebox

↓

Crystal growth by modified micro-pulling-down method

↓

Cutting and polishing of prepared single crystals

↓

Optical and luminescence characterizations

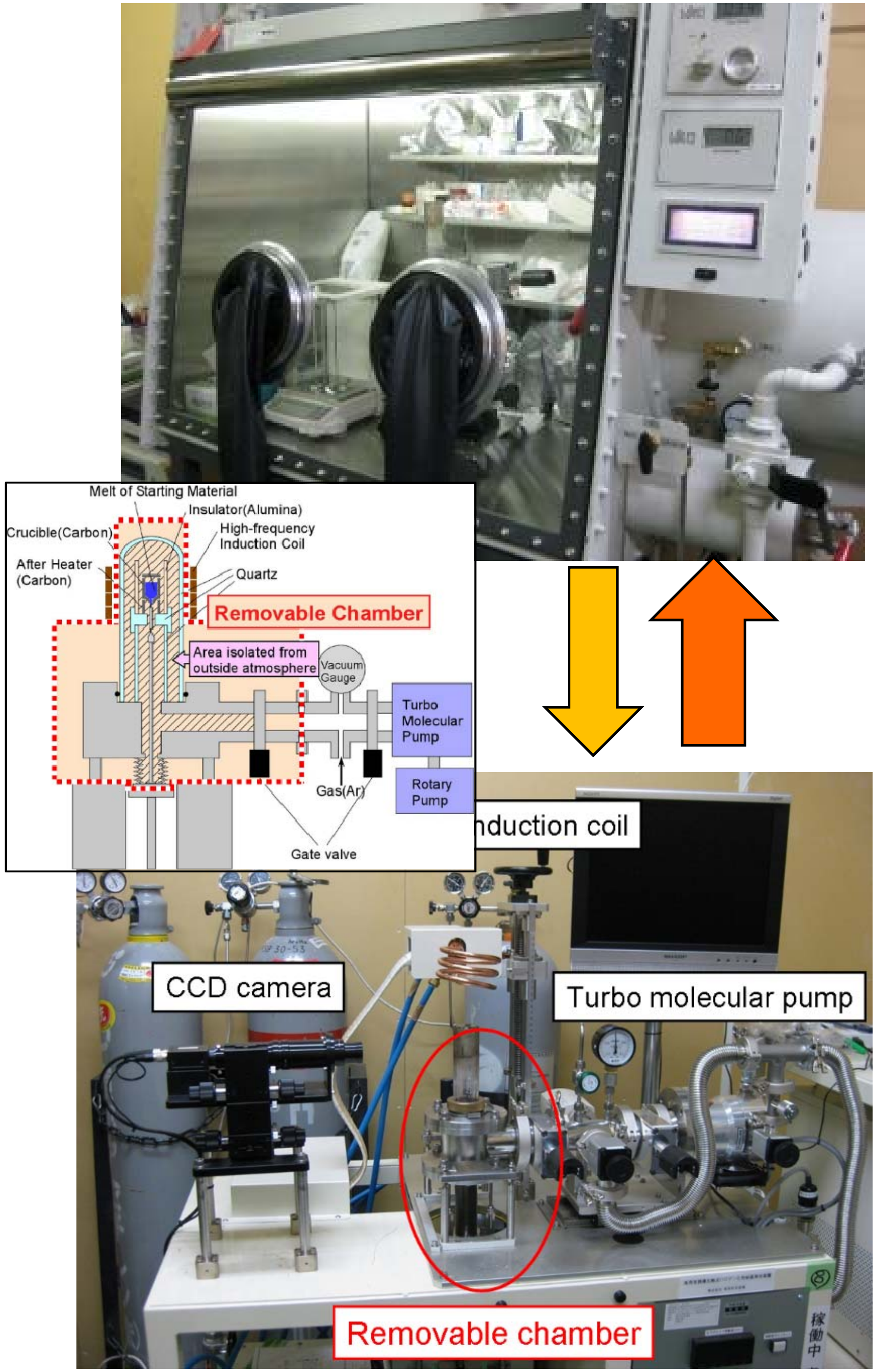

Crystal growth by μ-PD method

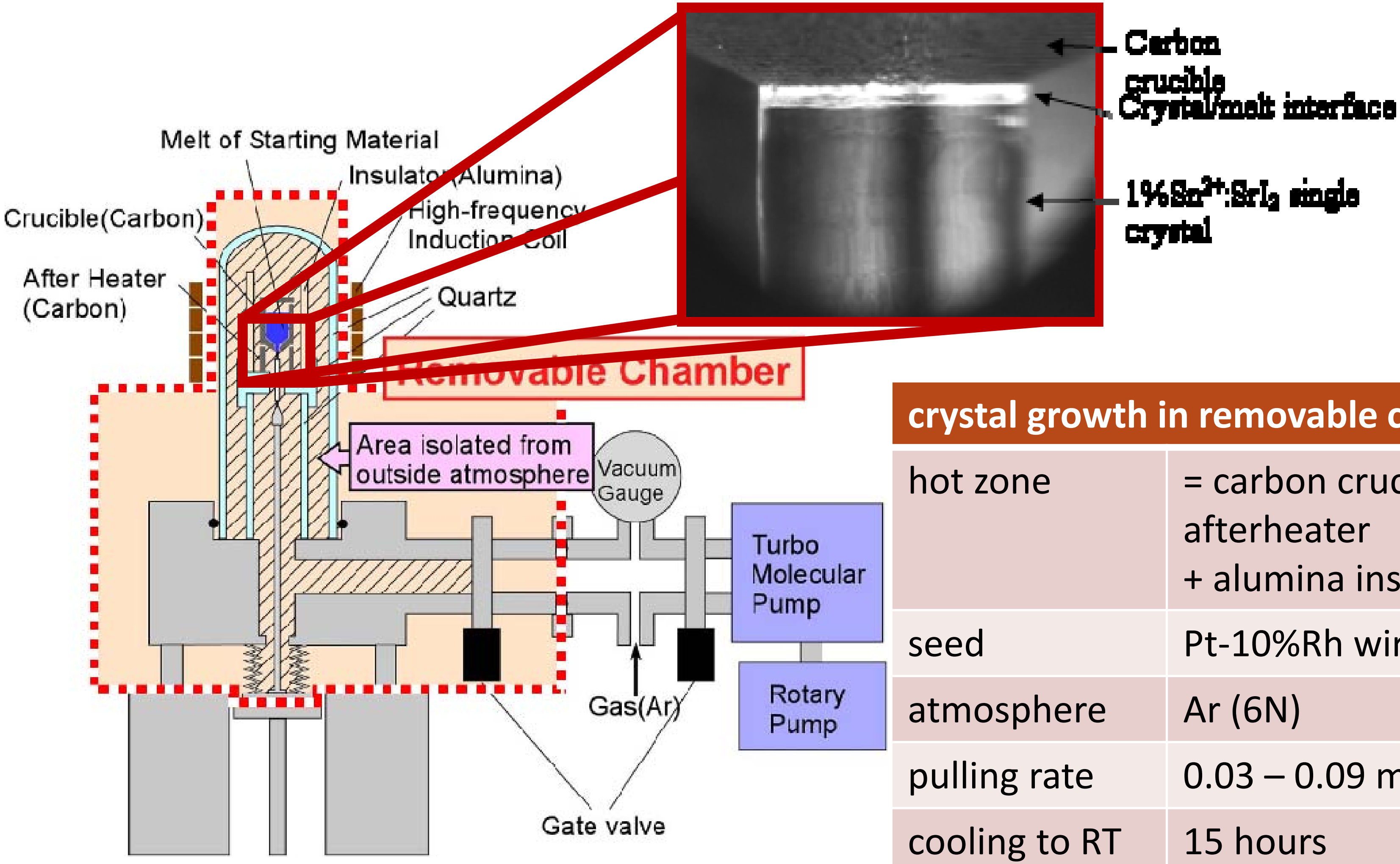

crystal growth in removable chamber	
hot zone	= carbon crucible, afterheater + alumina insulator
seed	Pt-10%Rh wire
atmosphere	Ar (6N)
pulling rate	0.03 – 0.09 mm/min
cooling to RT	15 hours

RE:RbPb$_2$Cl$_5$ (RE:RPC) for IR lasers

R. Král et al., Opt. Mater. 36 (2013) 214–220

as-grown RE:RPC hal. mPD in Japan

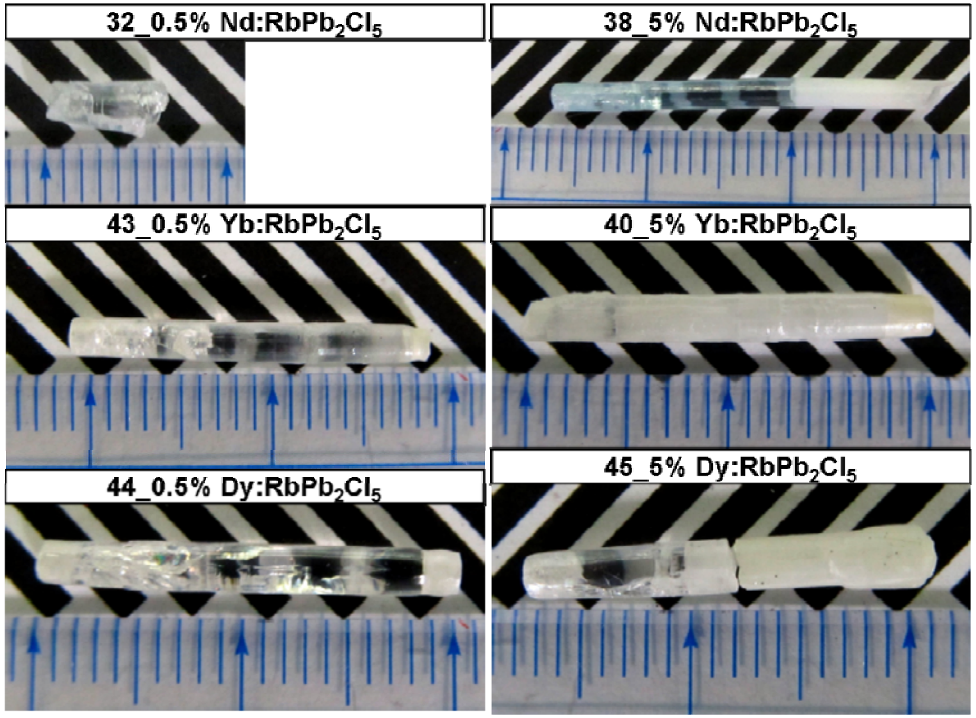

Radioluminescence, RT

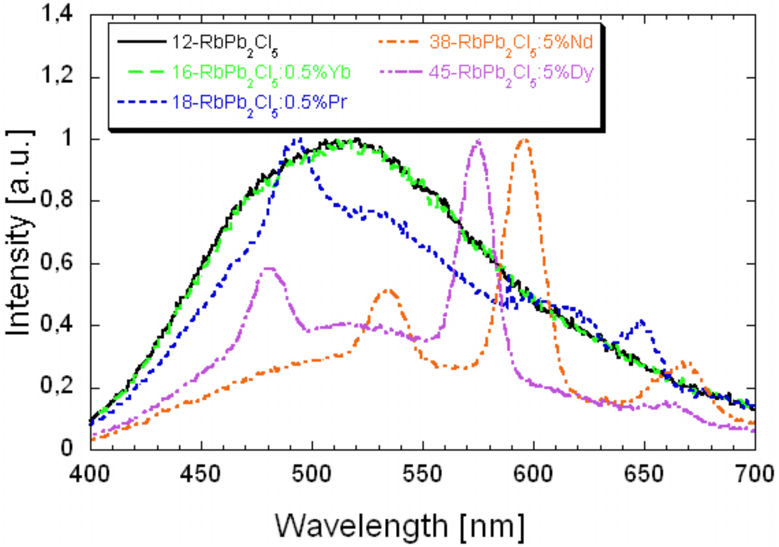

PL, PLE spectra, RT

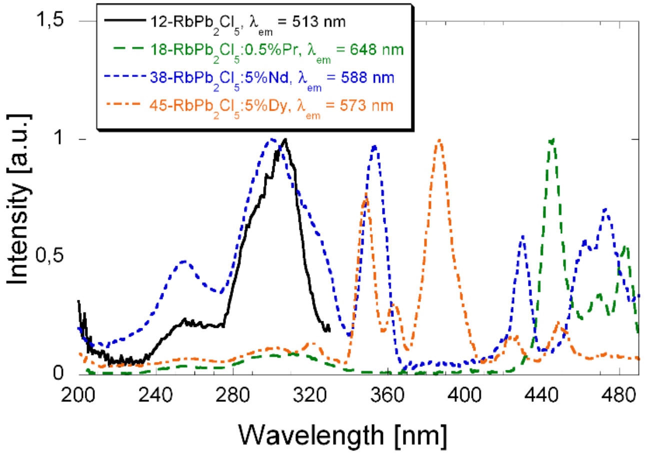

IR luminescence

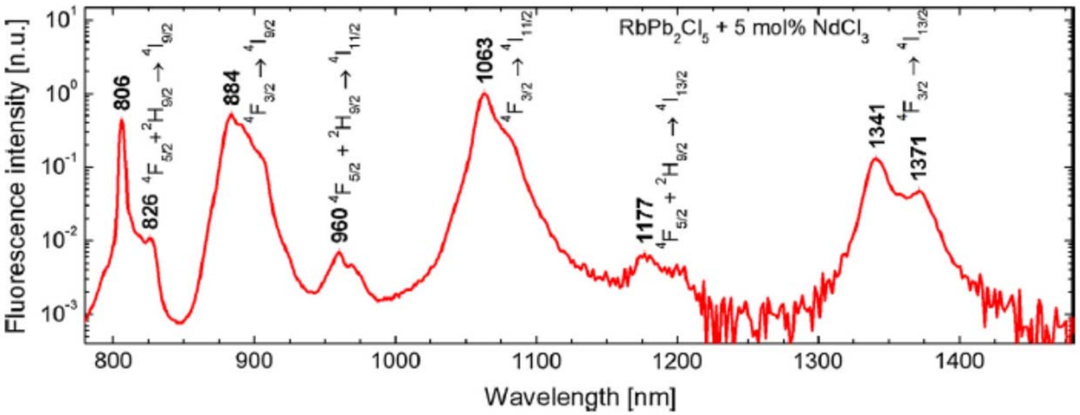

Thank you for your attention!

Summary

- Two approaches of Cs_2HfCl_6 synthesis were tested
- Application of zone refining requires improvements -> optimization of $HfCl_4$ partial pressure
- Growth of Cs_2HfCl_6 crystals by vertical Bridgman method
- polycrystalline with homogeneous grains (up to 10 mm)
- START (transparent, 97 mol% of Cs_2HfCl_6) and TAIL (nontransparent)

- decomposition over 760 °C, mass loss ca. 42 w% (TG-DSC)
- Cs_2HfCl_6, CsCl phase confirmed by XRD

- emissions related to host with maxima at 362 nm (RL, PL)
- 32 times more intense than standard BGO (RL)
- emission of Zr at 440 nm

- LY around 57000 ph/MeV, resolution 12%

Application of reaction agents

- N-based — NH_4X — solid
- Si-based — SiX_4 — g, l, s
- C-based — CX_4, COX_2, CO, $CH_{4-x}X_x$, — g, l, s
- HX-based — HX (HF, HCl, HBr, and HI) — all gaseous
- X-based, — X_2, — $F_2(g)$ and $Cl_2(g)$ — gaseous
  - $Br_2(l)$ — liquid
  - $I_2(s)$ — solid

Hygroscopicity

= “absorbing or attracting moisture from the air”

- connected to mass change

H_2O

sorption
- adsorption (surface)
- absorption (volume)

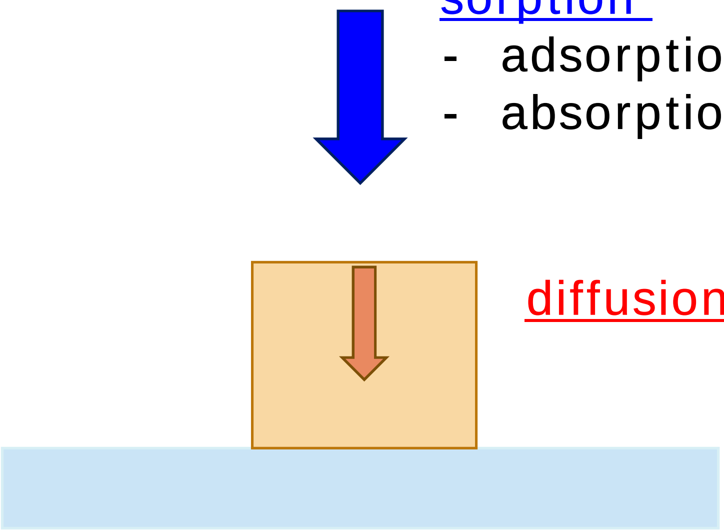

diffusion

physical adsorption
- Van der Waals forces
- fast (seconds)

chemisorption
- reaction
- formation of new compounds
- thermodynamics and kinetics

Reactions - example

$OH^- + HCl = Cl^- + H_2O$

$O_2^- + 2HCl = Cl^- + H_2O + 0.5\ Cl_2 + 0.5\ O_2$

$CO_3^- + 2HCl = 2Cl^- + H_2O + CO_2$

} **HX**

$OH^- + Cl_2 = Cl^- + HCl + 0.5\ O_2$

$O_2^- + Cl_2 = Cl^- + 0.5\ Cl_2 + O_2$

$CO_3^- + Cl_2 = 2Cl^- + 0.5\ O_2 + CO_2$

} **X_2**

Results - XRF

After zone refining

- opened x closed

Identification:

- Cs, Hf, Cl
- impurities: Zr < 0.03mol% (both)
- Na, Si, Al

Stoichiometric ratio Cs, Hf, and Cl						
System	**Element**	**1**	**2**	**3**	**4**	**5**
Opened	**Cs**	1.9	2.0	2.1	2.0	2.0
	Hf	1.0	1.0	1.0	1.0	1.0
	Cl	6.3	6.5	6.6	6.4	6.4
Closed	**Cs**	2.4	2.1	1.8	2.0	-
	Hf	1.0	1.0	1.0	1.0	-
	Cl	6.8	6.6	6.0	6.6	-

Cs_2HfCl_6, single crystal, START

PL, PLE spectra at RT

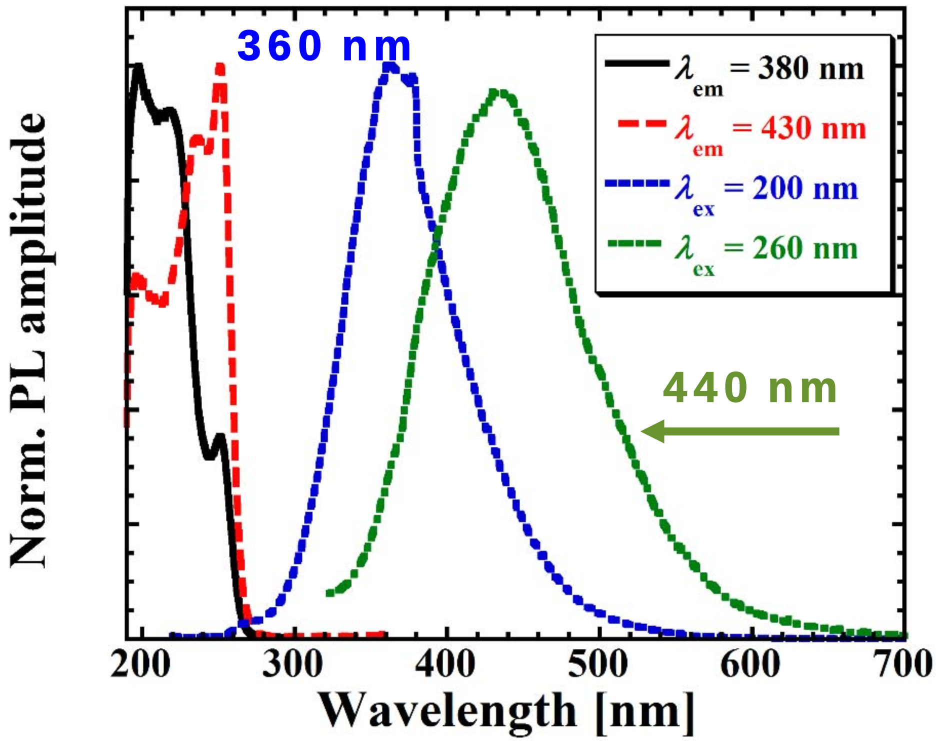

- ✓ **360 nm** – em. of STE in Cs_2HfCl_6
- ✓ **440 nm** – em. of STE of Zr impurity

PL decay at RT

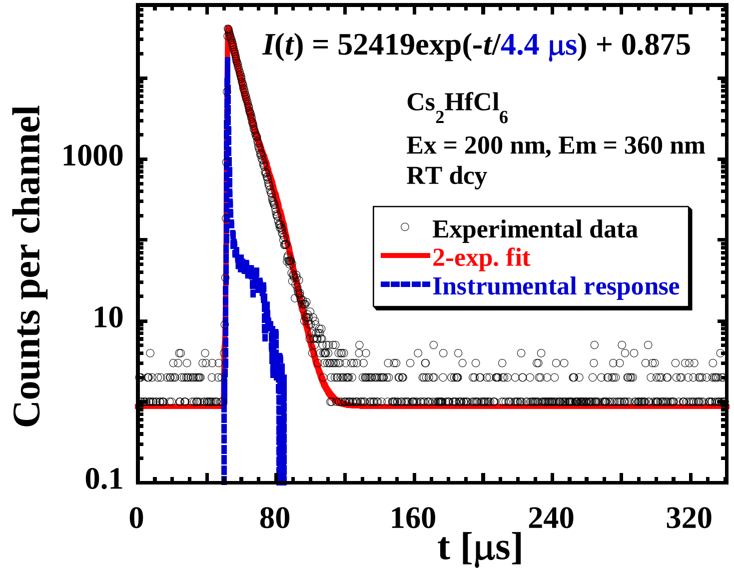

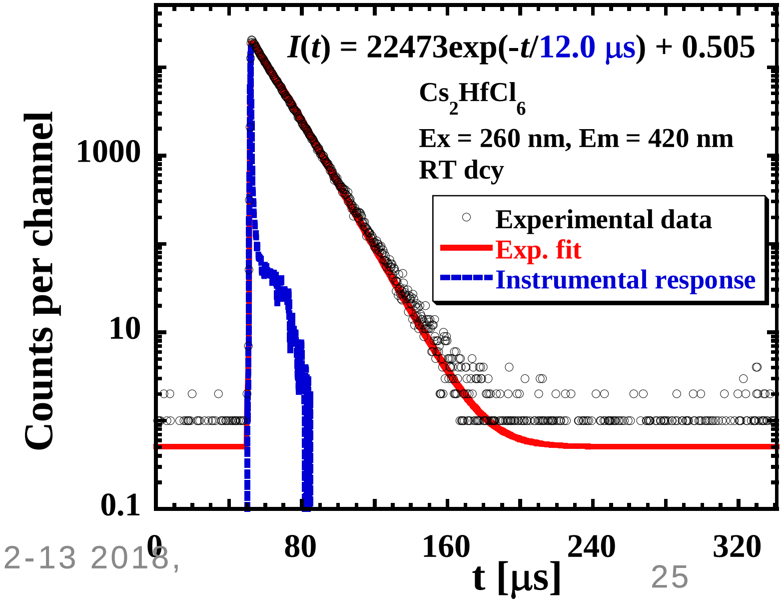

Cs_2HfCl_6 – single crystal

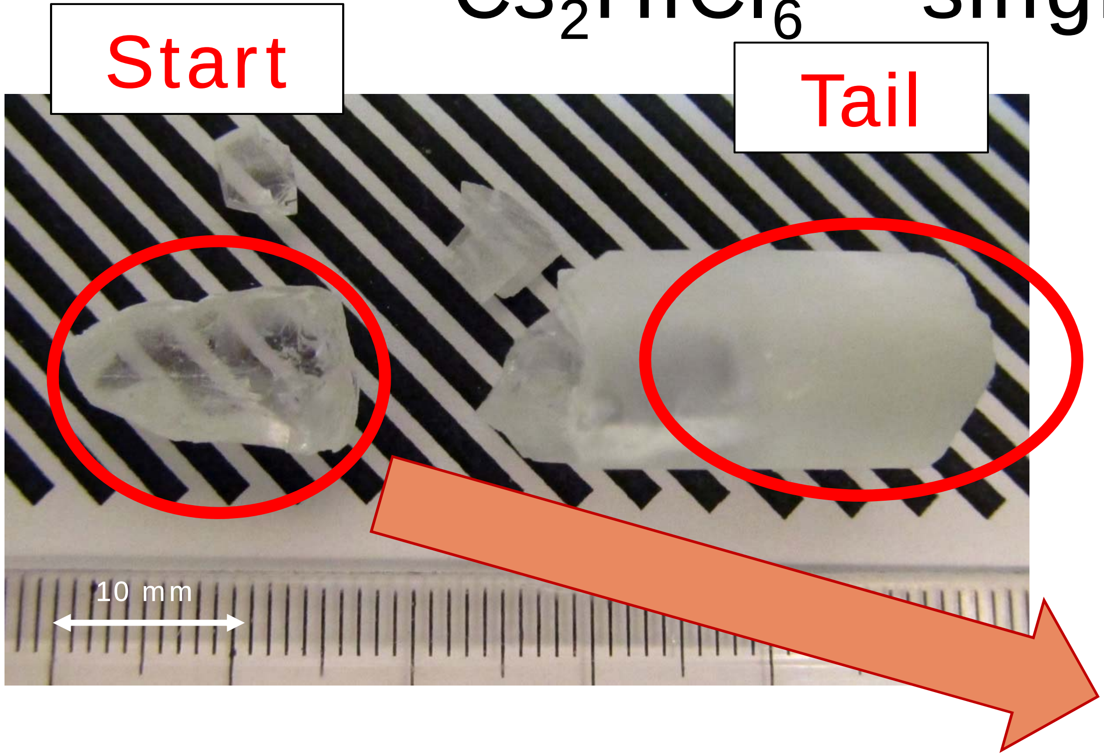

TG-DSC
XRD

TG-DSC

Radioluminescence

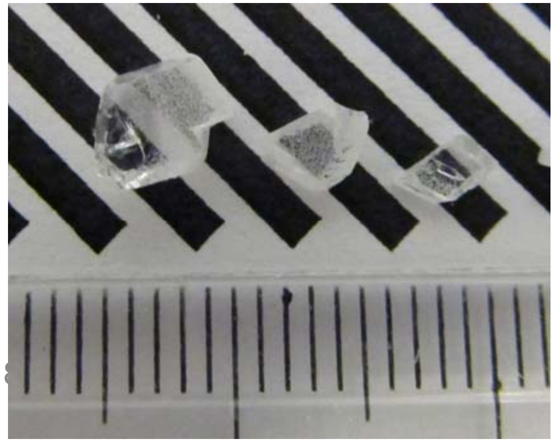

- 12 x 40 mm (D x L), colorless
- polycrystalline, homogeneous grains
- tip and bulk – transparent
- end – nontransparent

MS1

Light yield set up

The digitizer convert the voltage signal of the PMT into a vector of values (pulse shape). The pulse shape is integrated over time for a certain Gate length to obtain the light yield plot, from which we can distinguish Photo-peak and Compton shoulder. Comparing the photo-peak of a crystal with known intrinsic light yield (using the same set up and acquisition chain) we can estimate the light yield of an unknown crystal.
For a precise comparison, the surface state of the two crystal should be the same, as well as the geometry ratio.

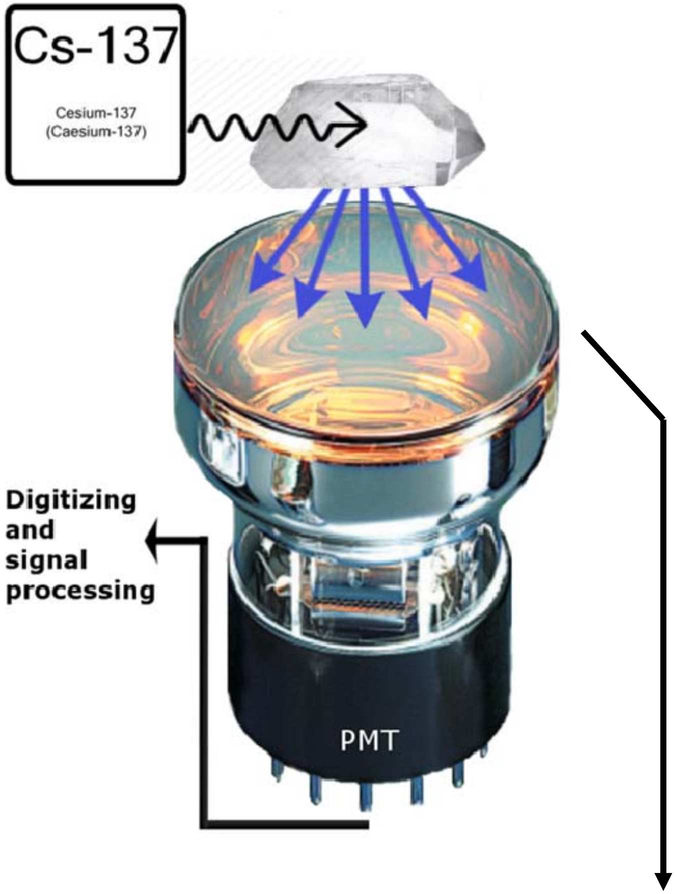

PMT quantum efficiency was precisely measured in the range of 350 nm to 550 nm

Slide 27

MS1 Matteo Salomoni; 19.12.2016

TG-DSC

Cs_2HfCl_6, single crystal, START and TAIL

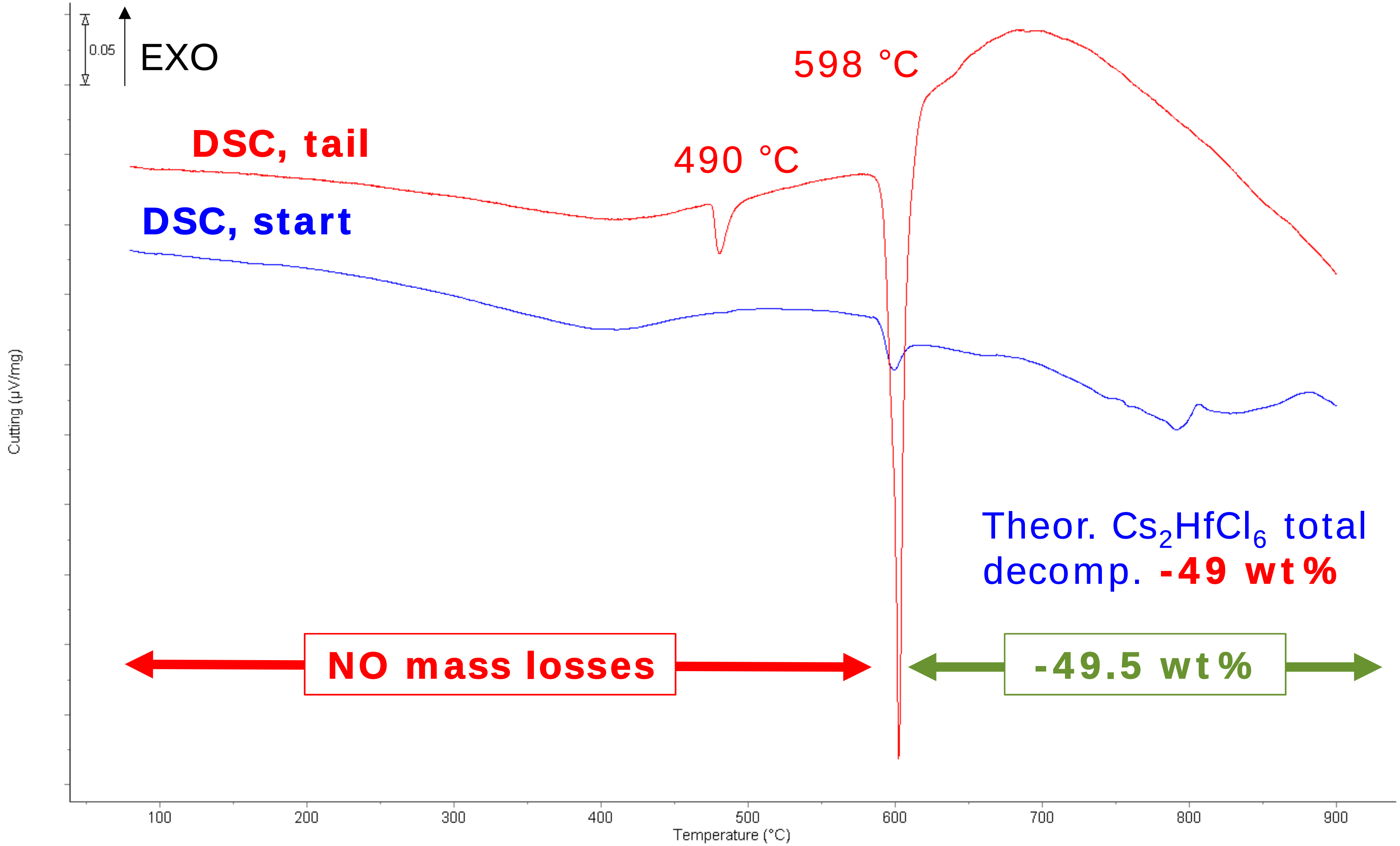

Synthesis – mass changes

Sample	Compound	Nominal mass [g]	Mass AFTER syn. [g]	Mass loss [%]
1	CsCl	10.5	-	-
	$HfCl_4$	10.0	-	-
	Cs_2HfCl_6	**20.5**	**16.8**	**18**
2	CsCl	21.0	-	-
	$HfCl_4$	20.0	-	-
	Cs_2HfCl_6	**41.0**	**38.3**	**7**

Prepared samples were subsequently purified using zone refining

Characterization methods

- X-ray fluorescence analysis (XRF)
- X-ray diffraction analysis (XRD)
- Simultaneous thermal analysis (TG-DSC)

After zone refining

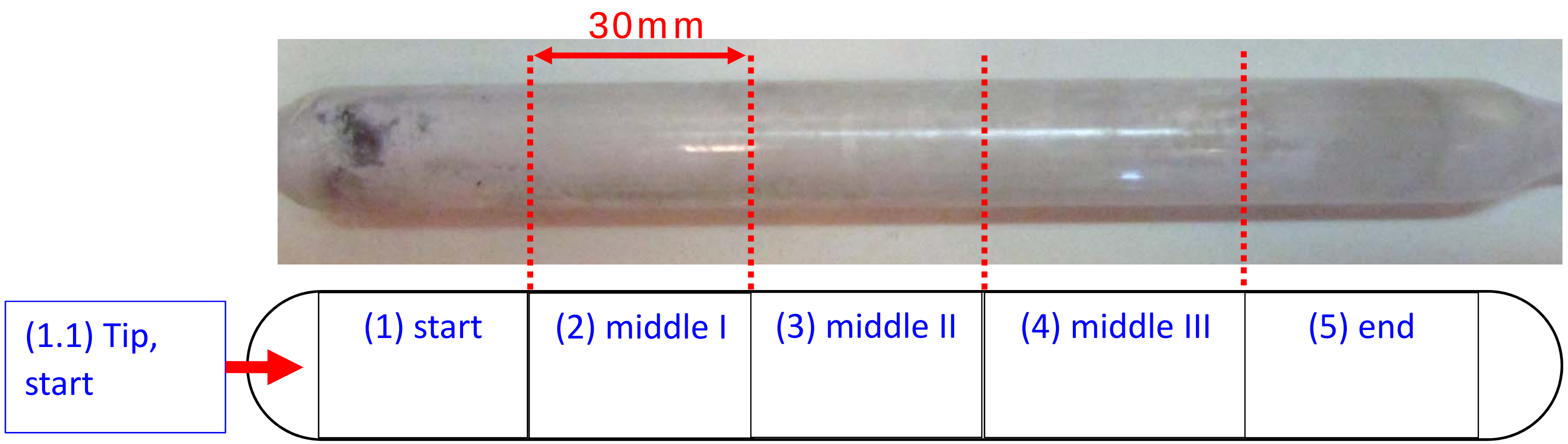

Single crystals K^+, Eu^{2+}:SrI_2

Growth direction →

66_SrI_2, undoped

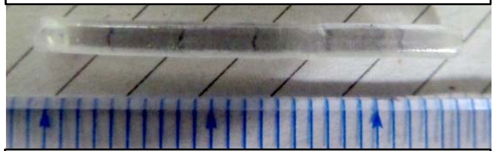

69_2%$EuCl_3$:SrI_2

81_0.9%Eu^{2+}:SrI_2

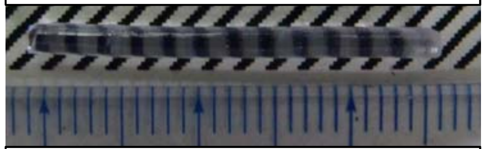

76_1%Eu^{3+}, 0.25%K^+:SrI_2

70_2%$EuCl_3$, 1%KI:SrI_2

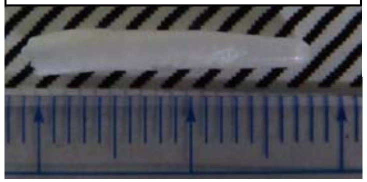

72_1%$EuCl_3$, 0.5%KI:SrI_2

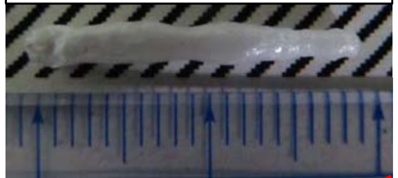

79_1%Eu^{2+}, 0.25%K^+:SrI_2

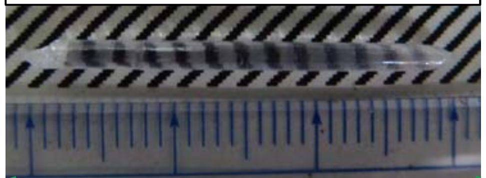

unstable growth, appearance of second phase during crystal growth

- doped with $EuCl_3$
- reaction when melting – I_2 gas evolving

stable growth

- doped with EuI_2

MS1

Characterization: Light yield

- The number of **photons collected at the PMT** surface from the Cs_2HfCl_6 emission is (ADC channel of the Single electron peak = 24, 10 dB attenuation and 160 Fc/LSB in the digitizer) 57145 ph / MeV

- The number of **photons collected at the PMT** surface from the LYSO emission is (ADC channel of the Single electron peak = 24, 10 dB attenuation and 160 Fc/LSB in the digitizer) 21206 ph / MeV

Slide 32

MS1 Matteo Salomoni; 19.12.2016

Raw crystal (bigger piece):

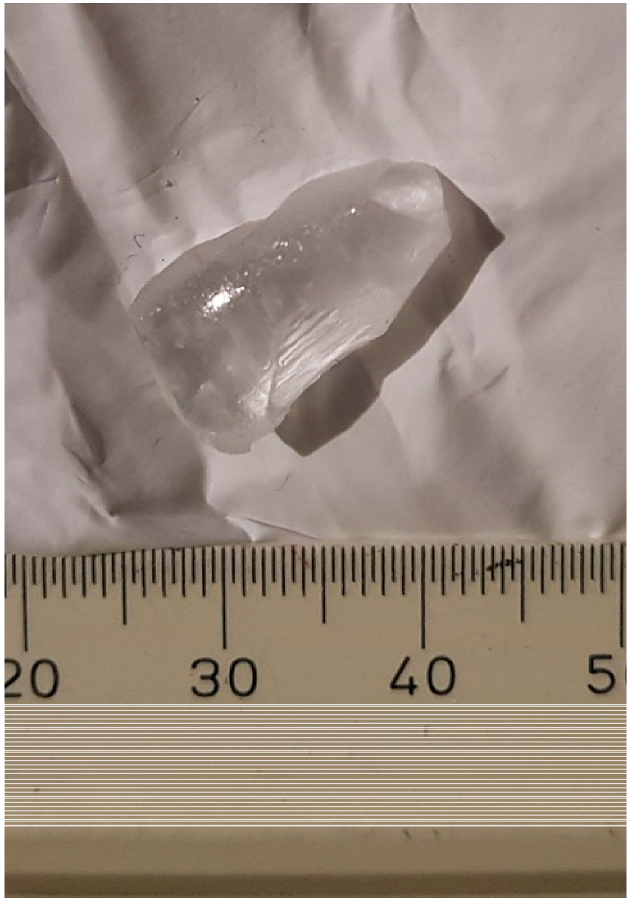

Cs_2HfCl_6 crystal, 1.5 x 0.6 x 0.7 cm^3 , ID #30.
Raw cut surface, Hygroscopic crystal.

Reference LYSO has different surface finish:
1 cm cube with polished surfaces.

QE of the PMT for Cs_2HfCl_6 emission spectrum was calculated to be 24.14%, close to the one calculated for LYSO -> 24.26%

Applications of scintillators

Medical application

PET, SPECT

High energy physics

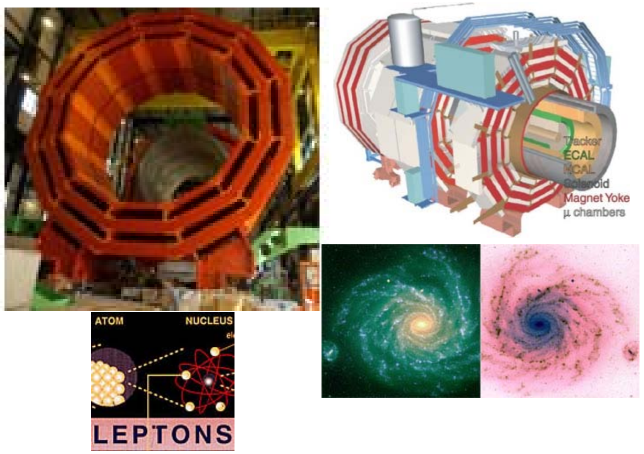

Particle physics, …

Security check

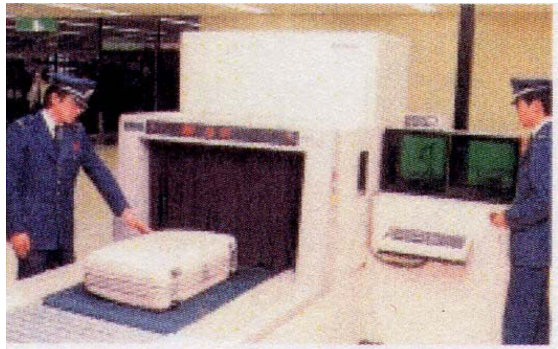

X-ray scanning

Nondestructive analysis

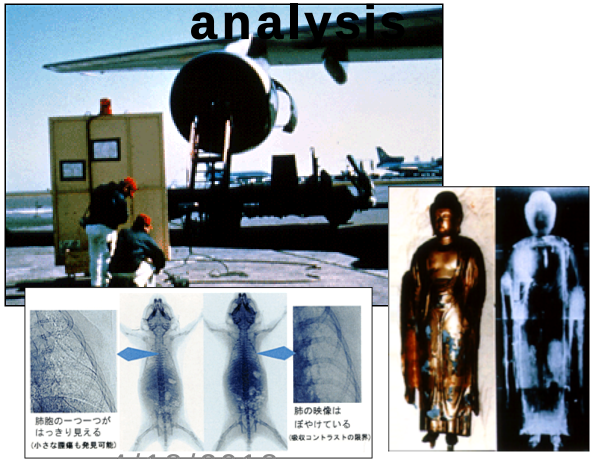

Computed tomography

Goods check

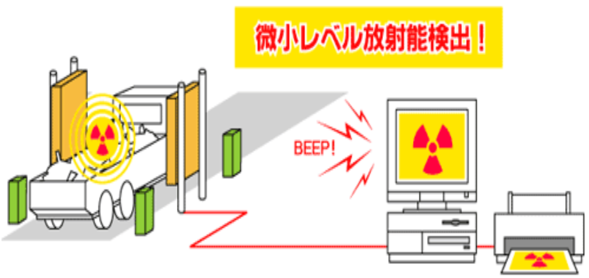

Remote detection

Other application

Geo- and environment